

# Phase-dependent electronic properties of monolayer and multilayer anthracene films on graphite [0001] surfaces

F. Bussolotti,<sup>1,2,\*</sup> S. W. Han,<sup>1,2</sup> Y. Honda,<sup>1</sup> and R. Friedlein<sup>1,2</sup><sup>1</sup>*School of Materials Science, Japan Advanced Institute of Science and Technology (JAIST), 1-1 Asahidai, Nomi, Ishikawa 923-1292, Japan*<sup>2</sup>*Research Center for Integrated Science, Japan Advanced Institute of Science and Technology (JAIST), 1-1 Asahidai, Nomi, Ishikawa 923-1292, Japan*

(Received 12 March 2009; revised manuscript received 12 May 2009; published 9 June 2009)

The evolution of the electronic properties of thin anthracene films on highly oriented pyrolytic graphite [0001] substrates as a function of temperature has been investigated using ultraviolet photoelectron spectroscopy. The change in the valence line shape with increasing substrate temperature has been univocally associated with the occurrence of different molecular orientations and structural phases (e.g., “flat-lying” mono- and multilayer films and a multilayer phase with a “standing-up” orientation). These thin-film phases are characterized by ionization energies varying up to 0.9 eV; the surface dipole and possibly to a minor extent polarization energy contributions are shown to be related to the specific molecular packing/molecular orientation and to the interplay between the molecule-molecule vs molecule-substrate interactions. Furthermore, for the monolayer system, a vibrational fine structure of the highest occupied molecular orbital (HOMO) is clearly revealed, thus allowing a detailed study of the HOMO hole-vibration coupling and the temperature-dependent broadening. Showing a large number of recently discussed contributions to the valence line shape, anthracene thin films emerge as “benchmark” systems to study the behavior of holes relevant for the charge transport in organic electronic devices.

DOI: [10.1103/PhysRevB.79.245410](https://doi.org/10.1103/PhysRevB.79.245410)

PACS number(s): 79.60.Dp, 72.80.Le, 68.35.Ja

## I. INTRODUCTION

Over the last three decades, organic molecular semiconductors have attracted increasing scientific attention due to their interesting chemical, optical, and electrical properties.<sup>1</sup> The possibility of processing large areas at low cost, light weight, mechanical flexibility, and high degree of freedom in molecular design, as ensured by the modern chemical synthesis techniques, makes organic molecular semiconductors suitable materials for the development of a wide range of solid-state electronic and optoelectronic devices such as thin-film field effect transistors,<sup>2–5</sup> photovoltaic cells,<sup>6,7</sup> and light emitting diodes.<sup>8</sup> Besides mainly application-oriented studies, considerable research efforts have therefore been devoted to understand the nature of charge transport mechanisms in organic molecular crystals and thin films of varying degrees of molecular order<sup>9,10</sup> as well to the electronic properties at the organic/metal interface.<sup>11–13</sup>

Organic semiconductors are characterized by weak intermolecular van-der-Waals interactions. Electronic states are in most cases localized around the single molecules leading to narrow (intermolecular) bandwidths as compared to their covalently bound inorganic counterparts and to a significant charge-vibrational coupling. Accordingly, the charge transfer is well described, at least at room temperature and in the absence of a high degree of structural ordering, in terms of thermally activated phonon hopping.<sup>14,15</sup> Charges localized at the femtosecond time scale experience the electronic polarization on neighboring molecules (intermolecular polarization),<sup>16</sup> the influence on the energy of the electron, or the hole being strongly correlated with the local structural environments in the bulk, at the surface, or at organic/substrate interfaces.<sup>17,18</sup> In addition, the injection or creation

of a charge in organic solids is accompanied by a strong intramolecular geometric relaxation that is directly related to the charge-vibrational coupling,<sup>14,15</sup> a key factor in determining the mobility in organic materials and for the occurrence of superconductivity under peculiar condition.<sup>19,20</sup> The study of charge localization and relaxation effects is therefore of prime importance for the understanding of charge transfer mechanism and the energy level positioning in organic thin-film structures and devices as well as for a correct interpretation of corresponding spectroscopic data. In this context, aromatic molecules with a simple chemical structure such as linear oligoacenes (i.e., anthracene, tetracene, and pentacene) play a major role since they function as model systems for investigations of fundamental electronic properties and the growth behavior of thin organic films, representing, at the same time, some of the most promising organic materials for technological applications.<sup>3–5</sup> In particular, a clear energy splitting of 0.3 eV of highest occupied molecular orbital (HOMO)-derived spectral feature has been observed in ultraviolet photoelectron spectra (UPS) of anthracene and pentacene thin films and has been attributed to the difference of polarization energies ( $P^+$ ) of surface and bulk molecules.<sup>17,21,22</sup> On the other hand, at the metal/organic interface, an enhanced screening related to the presence of the metallic substrate leads to further stabilization of the electron and hole energies and to narrowing of the transport gap with respect to the bulk value, as directly observed for the pentacene/Au and related organic/metal systems.<sup>23,24</sup> Variations in the ionization potential (IP) of organic thin films as a function of the crystal structure<sup>25</sup> and of the molecular orientation have also been reported;<sup>18</sup> the interpretation is mainly based on the dependence of  $P^+$  on the orientation and packing. Alternatively, according to recent experimental and

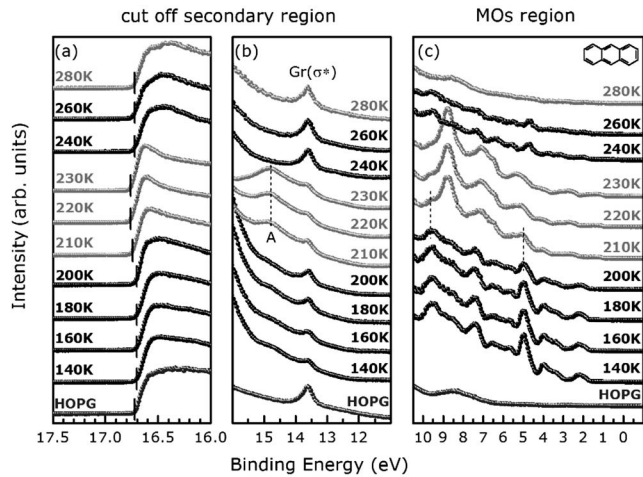


FIG. 1. Evolution of the anthracene film UPS spectra in the (a) and (b) cutoff and (c) molecular orbital regions as a function of the substrate temperature. The spectrum of the HOPG substrate is reported for comparison. The chemical structure of the anthracene molecule is shown in panel (c).

theoretical results,<sup>26,27</sup> the observed large dependence of the IP on the orientation has been attributed to differences in the surface dipole built into the molecular layers basically originating from the different intramolecular bonds exposed at the organic/vacuum interface. Despite the interpretative models, the IP site dependence has been known to contribute, besides the possible occurrence of band dispersion phenomena, to the broadening of the UPS HOMO spectral width in organic solids<sup>17,18,23,24,26,27</sup> with respect to the corresponding gaseous counterparts. Since for free, large organic molecules, vibrational progressions are sometimes observed, the charge-vibrational coupling and the intramolecular structural relaxation energy can be studied analyzing UPS gas phase spectra.<sup>14,28,29</sup> As for adsorbed molecules, vibrational satellites have been observed for the HOMO of phthalocyanine and pentacene monolayers on highly oriented pyrolytic graphite (HOPG) (Refs. 30 and 31) and on a metallic substrate.<sup>32</sup> These results clearly demonstrate the possibility of an effective study of the HOMO hole-vibrational coupling even for the condensed phase revealing important details on the origin of the intrinsic UPS line shape in organic thin films and on the role of the molecule/substrate interaction in governing the charge injection process.<sup>31,32</sup>

In order to shed light on the important issues addressed above, a detailed study of thin anthracene films on HOPG [0001] by UPS has been performed (see Fig. 1 for the schematic structure of the anthracene molecule). By employing a proper deposition/annealing strategy several structural phase transitions have been observed, the film thickness varying between mono- and multilayers. We are aiming to demonstrate that one can indeed distinguish between individual contributions related to the HOMO line shape, for the same molecule on the same substrate. This is made possible because their relative importance varies strongly with the molecular orientation. For this reason, anthracene may again become relevant for the understanding of thin-film electronic properties it was about 30 years ago in the influential work by Salaneck.<sup>17</sup>

## II. EXPERIMENTAL

UPS measurements have been performed in a new dedicated home-based setup, using unpolarized HeI photons ( $h\nu=21.218$  eV). Photoelectron spectra have been acquired using a SCIENTA SES-100 hemispherical analyzer integrating over  $\pm 6^\circ$  with respect to the spectrometer lens axes. The total instrumental energy resolution has been set to about 60 meV as indicated by the Fermi edge broadening of a sputtered copper surface. If not specifically indicated otherwise, the UPS data have been acquired at normal emission (polar emission angle  $\theta=0^\circ$ ). The vacuum level (VL) position has been determined from the secondary electron cutoff, with the sample being biased at  $-5$  V.

The HOPG substrate of ZYA quality (MDC-NDT Europe) has been cleaved in air just before introduction into the ultrahigh vacuum system (preparation chamber base pressure of  $2 \times 10^{-10}$  mbar) and annealed at 670 K for 12 h. The cleanliness of the substrate has been verified by UPS. The anthracene molecules have been inserted into a dedicated UHV chamber (base pressure of  $2 \times 10^{-10}$  mbar); separated from the preparation chamber by a gate valve, using a custom-built, differentially pumped feedthrough. *Prior* to deposition, the anthracene powder (Sigma-Aldrich, zone-refined,  $>99\%$ ) has been degassed at 400 K for 3 h, followed by a 12 h pumping cycle at room temperature. The anthracene deposition has been performed with the molecules held at about 295 K by opening the gate valve separating the evaporator from the preparation chamber. During the anthracene deposition the pressure in the preparation chamber remained stable at  $5 \times 10^{-8}$  mbar, being essentially the anthracene partial pressure. The total exposure to the molecules has been evaluated in Langmuirs ( $1 \text{ L}=10^{-6} \text{ mbar} \times \text{s}$ )

## III. RESULTS AND DISCUSSION

Multilayer anthracene films (30 L of total exposure) have been deposited onto the HOPG [0001] surface first, the substrate held at 140 K, and then stepwise annealed up to 280 K. UPS spectra as a function of substrate temperature, in the [Figs. 1(a) and 1(b)] secondary cutoff and [Fig. 1(c)] molecular orbital region, as well as the data of the HOPG substrate *prior* to deposition, are displayed in Fig. 1. The deposition of anthracene molecules leads to significant changes in the spectra, as compared with HOPG. In particular, a slight shift of the VL position of 20 meV toward lower binding energy is measured [Fig. 1(a)]. As shown in Fig. 1(b), the intensity of a sharp peak, denoted as  $\text{Gr}(\sigma^*)$ , at a binding energy of 13.6 eV originating from the conduction band of the HOPG [0001] surface is significantly reduced. Additionally, several adsorbate-induced features appear in the binding energy range of [1–10] eV [Fig. 1(c)] that are related, as clarified in the following discussion, to anthracene molecular orbitals.

Note that, as reported previously,<sup>17,21</sup> the surface molecular mobility is reduced at low temperatures preventing nucleation and the occurrence of an island growth mode, as generally observed in the case of planar molecules deposited near room temperature on metallic and nonmetallic

substrates.<sup>32,33</sup> Under the hypothesis of such a homogenous, layered growth a thickness of  $\sim 3$  nm is estimated on the basis of the attenuation of the  $Gr(\sigma^*)$  signal (at a kinetic energy of 8 eV considering the biasing voltage) assuming an electron mean-free path of  $\sim 2$  nm.<sup>34</sup>

Upon initial annealing (up to 200 K), a slight reduction in the intensity of the adsorbate-induced features is observed [Fig. 1(c)]. This decrease coincides with the increase in the substrate-related peak  $Gr(\sigma^*)$  [Fig. 1(b)], while the VL position remains unaffected by the thermal treatment [Fig. 1(a)]. These observations indicate the occurrence of a progressive molecular desorption resulting in a reduction in the film thickness. By annealing at higher temperatures (above 200 K), a strong variation in the spectral shape of the adsorbate related features is observed [Fig. 1(c)]. Such variations in the electronic properties are certainly related to structural and morphological changes where details may be understood by comparison with other published oligoacene systems<sup>33</sup> or as an educated guess even if, as in our experiments, no direct structural assignment is available.

Between 210 and 240 K, the VL position gradually increases by 60 meV, accompanied by the appearance of a peak at 14.8 eV, denoted as A [Fig. 1(b)]. Similar to the substrate-related feature  $Gr(\sigma^*)$ , such peaks close to the secondary electron cutoff originate from resonances above the vacuum level experienced by the outgoing secondary electrons. In analogy to pentacene,<sup>18</sup> this peak may well originate from a high density of states in the conduction band related to a particular crystalline structure of the anthracene film. Interestingly, raising the temperature between 210 and 240 K, the intensity of A follows the temperature while  $Gr(\sigma^*)$  remains essentially unaffected. This indicates the absence of any significant molecular desorption. At the same time, the intensities of the molecular derived features vary only slightly [Fig. 1(c)]. The peculiar evolution of spectra between 210 and 240 K can easily be interpreted in terms of a standard phase transition during which all of the external thermal energy is used in the progressing crystallization of the new film structure thus quenching the occurrence of molecular desorption. In addition, most of the VL shifts (40 meV of the total increase of 60 meV) is observed at the beginning of the crystallization process at 210 K. In this context, it should be noted that such changes may result from the average of the signals collected from regions characterized by different film morphologies and different VL positions. The presence of such coexisting regions is supported by the UPS data reported in Fig. 1(c) where some of the higher-intensity features of the low-temperature multilayer phase are still visible in the 210 K spectra [as indicated by dashed lines in Fig. 1(c)] and quenched with the progression of the phase transition.

This “high-temperature multilayer” phase is evidently unstable upon additional further annealing due to the possible occurrence of molecular desorption, as clearly indicated by the suppression of A and the increase in  $Gr(\sigma^*)$ , observed at 240 K [Fig. 1(b)]. At the same temperature, the VL position shifts by 20 meV (up to the HOPG value), while the overall intensity and the energy distribution of the anthracene related peaks are newly modified with respect to the high-

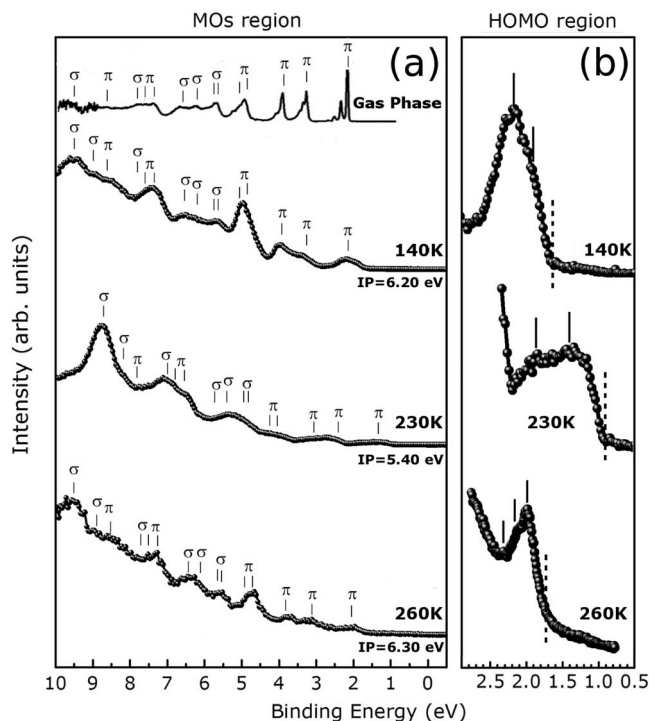


FIG. 2. (a) UPS spectra of the “flat-lying” multilayer (140 K), “standing-up” multilayer (240 K), and monolayer anthracene phases (260 K). The gas phase data (acquired at 60 eV, see Ref. 29) are included for comparison. The gas phase spectrum has been aligned with respect to the HOMO position of the “flat-lying” multilayer film. The orbital character of the molecular features is indicated. (b) UPS HOMO region as acquired for the different anthracene phases. IP values are reported for each phase as well.

temperature multilayer crystalline phase. This step is consistent with the disappearance of overlayers constituting the multilayer film such that only a mono- or possibly a sub-monolayer remains. More evidence will be discussed later. Upon even further annealing, the intensity of the molecular features is gradually suppressed with the temperature. In particular, at 280 K a complete recovery of the HOPG UPS line shape is observed, indicating the complete desorption of anthracene molecules from the supporting substrate.

According to the UPS data reported in Fig. 1, the effect of annealing on the electronic structure of the anthracene films can be summarized by identifying three main temperature ranges: [140–200 K], [210–230 K], and [240–260 K], where different photoelectron emission line shapes related to particular film morphologies and structures are observed. For a more detailed discussion, spectra acquired at 140, 230, and 260 K are plotted in Fig. 2(a) and have been selected to discuss electronic properties of the low- and high-temperature multilayer and monolayer phases, respectively. The gas phase anthracene UPS valence-band spectrum is shown for comparison.<sup>29,35</sup> In order to derive the  $\pi(\sigma)$  molecular orbital character of the adsorbate-induced features, gas and condensed phase UPS spectra have been aligned with respect to the HOMO peak position. Ionization potentials have been derived as the energy difference between the HOMO onset as indicated by the dotted lines in the magnified HOMO scans of Fig. 2(b) and the corresponding



vacuum level positions. As will be shown in detail below, the good correspondence to the gas phase data [Fig. 2(a)], beside rigid shifts allows exclusion of the coexistence of various regions characterized by a different local aggregation state and distinguishable values of the intermolecular polarization energy. Any variation in the shape and energy of the HOMO line between the three phases shall therefore entirely be ascribed to properties related to a particular film morphology and structure for each phase.

The HOMO line observed for the low-temperature multilayer phase at 140 K [Fig. 2(b)] shows a small shoulder at the low-binding-energy side. The occurrence of that feature may be explained in terms of different  $P^+$  values as experienced by the molecule at the surface (high-binding-energy component) and in the bulk (low-binding-energy component) of the thin film. In particular, the measured values of the energy splitting of 0.3 eV and of the IP of 6.2 eV are perfectly coincident with those obtained for anthracene thin films deposited onto polycrystalline gold substrates<sup>17</sup> where shifts related to differences between the surface and bulk polarization energies have been suggested on the basis of experimental data.<sup>17</sup> If the splitting would be due to a different  $P^+$  for the surface and bulk, a similar energy separation should be observed for *all* of the molecular features. As claimed already above, however, this is not the case for the present low-temperature multilayer phase, in view of the good matching between the data for the gas and condensed phases. The lack of polarization splitting for the high-binding-energy features could be argued as related to the low-intensity ratio between the surface and bulk components [as visible in 140 K HOMO line of Fig. 2(a)], combined with some broadening and a superposition of anthracene peaks related to different orbitals. In order to test this hypothesis, 120 L of anthracene molecules have independently been deposited, with evaporation conditions similar to those employed for the 30 L film. The corresponding UPS spectra are compared in Fig. 3(a). Importantly, increasing the film thickness only affects the line shape of the HOMO where the intensity of the low-binding-energy component is increased for the thicker film. The energies of all features, on the other hand, are not modified. The main point to note is that even in the presence of a well-defined HOMO energy separation, still there is no splitting observed for the high-binding-energy components of the 120 L film. The HOMO splitting shall therefore not be ascribed to the site dependence of the polarization energy,  $P^+$ . In this context, it is worth noting that this result is consistent with conclusions derived recently from high-resolution core level photoelectron experiments performed on layered aromatic molecular materials. For the thin films investigated, the absence of any appreciable surface core level shift suggested a strong reconsideration of surface polarization effects for the final state of the photoelectron emission process.<sup>36</sup> Note that a possible identification of the HOMO low-binding-energy shoulder as signal from a monolayer partially covering the surface is suggested from the similar binding energy position [see 260 K spectrum in Fig. 2(b)] but shall be excluded from the thickness-dependent spectra shown in Fig. 3(a). A monolayer may be present in case of a “layer+island” growth mode. For such a morphology, the signal from the monolayer is expected to be

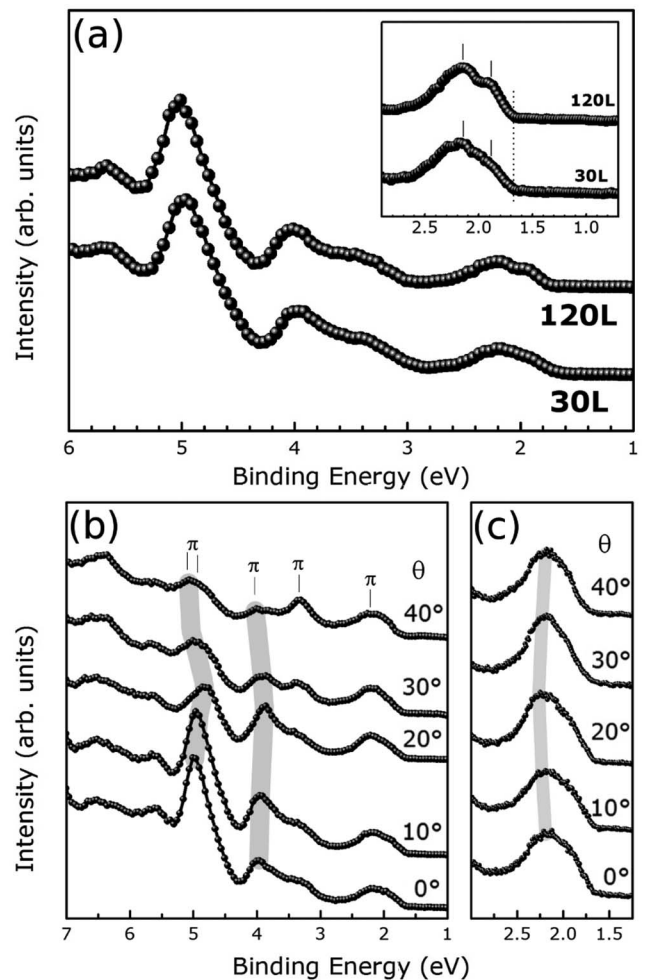


FIG. 3. (a) Comparison between the UPS spectra of anthracene multilayer films at 140 K prepared with a different nominal exposure (30 and 150 L). (b) Evolution of the UPS spectrum of the low-temperature anthracene multilayer phase (30 L) as a function of the polar emission angle  $\theta$ . (c) Magnification of the HOMO region of spectra reported in panel (b). The shadow area indicates the dispersive behavior of anthracene-derived electronic states (see text for further details).

reduced or at least stable when the islands grow larger, in contrast with what is observed in the present case, thus allowing to rule out this explanation. On the basis of the presented results a different, more suitable explanation for the observed HOMO splitting should therefore be found considering the peculiar structural properties of the low-temperature multilayer phase.

As shown in Fig. 2(a), the valence band of the extended region supports the idea that the long axis of the anthracene molecules in this low-temperature multilayer film is oriented parallel with respect to the substrate surface (“flat-lying” geometry). The spectrum is in fact widely dominated by the  $\pi$  orbital contributions whose photoelectron emission cross section at normal emission is enhanced for low photon incident angles with respect to the molecular plane,<sup>37–39</sup> the photon incident angle with respect to the substrate plane being 20° in our experimental configuration.

As observed in the case of the “flat-lying” pentacene thin-film structure with a herringbonelike molecular packing perpendicularly to the substrate plane,<sup>33</sup> and also predicted for many other pentacene polymorphs,<sup>40</sup> an energy splitting may well relate to the presence of two inequivalent molecules per unit cell. According to this picture, the HOMO line shape observed for the as-deposited anthracene multilayer film may display the signature of electronic bands dispersing perpendicular to the longer molecular axis originating from the  $\pi$ - $\pi$  overlap between the molecules in adjacent molecular planes. This idea is confirmed by the evolution of the UPS spectra acquired at different polar angles  $\theta$  reported in panels b and c of Fig. 3. A clear dispersive behavior of  $\pi$ -derived states [Fig. 3(b)] as well as of the HOMO centroid [Fig. 3(c)] is observed. This result is consistent with the occurrence of band dispersions (with a bandwidth of up to 0.3 eV) most likely perpendicularly to the film surface, even if dispersive contributions along the parallel direction cannot be excluded. Note that in the case of the similar pentacene “flat-lying” phase no significant HOMO dispersion has been observed by UPS as a function of  $\theta$  but has been by changing the photon energy at normal emission.<sup>33</sup> This is a consequence of the strong anisotropic out-of-plane character of the band dispersion. The occurrence of dispersions for deeper valence states that are larger than for the HOMO has already been observed in other layered organic films.<sup>41</sup> Our observation confirms the crucial role played by the molecular packing in determining the band dispersion in thin, crystalline organic films.

A very similar spectral intensity distribution is observed for the film annealed at 260 K [Fig. 2(a)] that can accordingly also be associated with a “flat-lying” phase. Remarkably, as shown in Fig. 2(b), the HOMO peak exhibits at least three components equally spaced with 170 meV. This fine structure originates from the HOMO hole-vibrational coupling that can only be resolved for well-ordered, ultrathin organic films.<sup>42</sup> Thus the present observation represents a clear signature of the successful preparation of a well-oriented and uniform anthracene film of monolayer (or possibly submonolayer) thickness. The appearance of the “flat-lying” monolayer phase at temperatures above 240 K may be naturally associated to desorption of overlayers of upright standing molecules if the flat orientation is the most stable structural form at this temperature. Like for other similar oligoacene systems,<sup>18</sup> it is very much possible that the layer nearest to the substrate pre-existed already with a flat-lying molecular orientation at all temperatures and that molecules associated with this first layer did not tilt during the phase transition between the low- and high-temperature multilayer phases. This information cannot be obtained with the surface-sensitive UPS technique.

The relative weight of the  $\sigma$  and  $\pi$  orbitals is reversed in the case of the high-temperature multilayer phase obtained at an intermediate temperature of 230 K [Fig. 2(b)] indicating a “standing-up” adsorption geometry; the long molecular axis now nearly aligned along the surface normal. As already discussed from the analysis of the secondary electron region [see peak A in Fig. 1(b)], this phase is characterized by crystalline ordering. In analogy to a similar pentacene polymorph,<sup>18</sup> the splitting and broadening of the HOMO-derived spectral feature at 230 K may originate from dispers-

ing bands as well. The present separation between HOMO bands of about 0.5 eV equals to the value reported for another “herringbone packed” thin-film phase of oligoacene molecules.<sup>18</sup>

Another important point relates to the strong variation in the IPs in between the three phases related to the different structures and film morphologies. In particular, a large reduction in the IP of 0.9 eV is observed at the transition from the low-temperature to high-temperature multilayer phases associated with the change in molecular orientation (from “flat lying” to “standing up”). The present observation may be rationalized, in principle, by invoking (i) a higher screening contribution from the substrate,<sup>23,24</sup> due to a progressing reduction in the film thickness as a function of the annealing temperature, (ii) a different intermolecular screening contribution, expressed as  $P^+$ , related to the variation of the molecular packing,<sup>18,25</sup> or (iii) differences in the built-in surface dipole of the molecular layers basically originating from different orbitals exposed at the vacuum/organic interface, as proposed only recently on the basis of photoelectron emission results and density functional calculations, for “flat-lying” vs. “standing-up” oligothiophene phases.<sup>26</sup> For large polyaromatic hydrocarbons, these dipoles vary by up to 0.8 eV depending on the orientation.<sup>43</sup>

While all of these three mechanisms are expected to be present, only one of them might be dominant. Mechanism (i), which commonly justifies a large IP thickness dependence in the case of organic layers deposited onto metallic substrate,<sup>23,24</sup> does not explain the large variation observed in the present data because of the relatively low dielectric constant of the graphite substrate.<sup>44</sup>

Polarization energies for a large number of organic films have been surveyed by Sato *et al.*<sup>22</sup> to yield variations within 0.4 eV but are large only for a few very special cases. An explicit dependence on the crystal structure of perylene of 0.3 eV (Ref. 25) may actually represent an upper limit for any eventual molecular packing dependence of  $P^+$ . Mechanism (ii) shall therefore be ruled out to explain the IP change of 0.9 eV as well. Consistently, the anthracene data may be mainly understood on the basis of mechanism (iii). In particular, in analogy with a simple picture proposed for similar  $\pi$  conjugated molecules, in the “flat-lying” phase of anthracene film the electron-rich (negative)  $\pi$  orbital side delocalized over the molecular plane is exposed at the vacuum interface thus determining a high value of the ionization potential. Similarly, in the “standing-up” phase the positive H side of the  $\sigma$  C-H bond is responsible for a lower IP. Furthermore, IPs within 50 meV similar for the low-temperature multilayer (140 K) and monolayer (260 K) phases [see the corresponding HOMO onset position in Fig. 2(b)] confirm the crucial role of the surface dipole in determining ionization energies and the energetic alignment at the vacuum/organic interface. Our results represent therefore a clear confirmation of the model put forward by Duhm *et al.*<sup>26</sup> related to the built-in surface dipole for the determination of the IP.

With the large variation in electronic properties of the multilayer structures, and given also the rather simple chemical structure of the molecule, the anthracene/HOPG [0001] system invites further theoretical investigations in this sense.

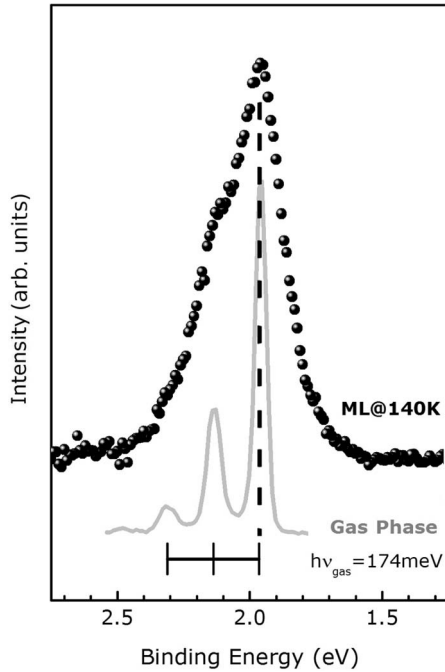


FIG. 4. The normal emission HOMO UPS spectrum of the anthracene/HOPG [0001] monolayer measured at 140 K, after subtraction of a smooth background, compared with the gas phase spectrum (Ref. 28). The gas phase spectrum has been aligned with respect to the HOMO position of the monolayer film measured at 140 K.

At the same time, the successful preparation of well-defined, “flat-lying” anthracene monolayer thin films at 260 K, as indicated by the HOMO fine structure [Fig. 2(b)], opens the possibility to study, by comparison with similar systems,<sup>31</sup> the role of the molecule-substrate interaction in influencing the intramolecular relaxation at the interface, charge injection, and transport mechanism in devices.<sup>45</sup> In particular, by considering the flat adsorption geometry, the  $\pi$ - $\pi$  interactions between graphite and molecules can also be considered to be representative of the situation occurring in the bulk of oligoacene materials.<sup>31</sup>

The evolution of the HOMO line shape of the monolayer phase has been studied as a function of the substrate temperature (260 and 140 K). In Fig. 4, the HOMO line shape of the anthracene film cooled at 140 K is shown and compared to the corresponding gas phase data (acquired with 60 eV photons<sup>29</sup>) after a proper subtraction of a smooth background. The spectra have been aligned with respect to the position of the maximum of the first vibrational peak. As already pointed out in the discussion above, the HOMO line shape of the monolayer anthracene film results from the superimposition of at least three different components that are, in analogy with the corresponding gas phase results, associated with vibrational levels of the ionized state reached in the direct transition between the ground and final states of the photoelectron emission process.<sup>29</sup> These satellites are related to the intramolecular coupling of the photohole to C-C stretching modes and indicate the persistence of a molecular character in the anthracene monolayer. Any modifications, in terms of energy separation and relative intensity of the vibra-

tional satellites, as compared to the corresponding gaseous counterparts, can essentially be ascribed to be caused by the molecule-substrate interaction, as previously discussed for the case of pentacene/HOPG [0001] on the basis of experimental<sup>31</sup> and theoretical studies.<sup>45</sup> Different to the pentacene film, a perfect matching of the energy separation of main satellites of 174 meV of the gas phase and monolayer spectra indicates clearly the reduced effect played by the HOPG substrate in influencing the geometrical intramolecular relaxation. This conclusion is further supported by the observation of only a very small angular dependence in  $\theta$  of the intensity ratio of the vibrational satellites (within 10% of the integrated value, spectra not shown) for angles of up to 45° from normal such that the Franck-Condon principle is fulfilled. The angular dependence is similar for both temperatures (260 and 140 K),

The vibrational progression of the HOMO line has been simulated using three Voigt components, with the energy separation kept fixed at the gas phase value ( $h\nu = 174$  meV). In order to take into account the slight angular dependency and to reduce the uncertain in the deconvolution procedure, spectra at different angles have been summed up and deconvoluted. In case of harmonic oscillators, the intensity of vibrational satellites follows a Poisson distribution,  $I_n = S^n e^{-S} / n!$ , where  $I_n$  are the intensity of the  $n$ th vibrational satellite and  $S$  is the Huang-Rhys factor.<sup>14</sup> According to this model, the intramolecular reorganization energy,  $\lambda$  is given by  $\lambda \approx 2Sh\nu$ . The results obtained in this way for the monolayer at 260 and 140 K are reported in Figs. 5(a) and 5(b), respectively. For both temperatures, the angle-integrated spectra are well reproduced by adjusting the Gaussian ( $W_G$ ) and Lorentzian ( $W_L$ ) contributions to the broadening, using three components. Finally, a Huang-Rhys factor value  $S$  of 0.430 is derived.

As with regard to the Voigt-like line shape of individual vibrational components, Gaussian and Lorentzian contributions vary with the substrate temperature. Contributions due to a Lorentzian broadening are minor and increase only slightly from 74 to 85 meV with the temperature. A pronounced Lorentzian-like low-binding-energy tail is absent, indicating a long lifetime of the photohole that does not delocalize to the substrate on the time scale of a few femtoseconds.<sup>31,42</sup> Gaussian contributions increase from 140 meV at 140 K to 160 meV at 260 K. A broadening on the low-binding-energy side with temperature, as observed here, may possibly be attributed to a “hot band” excitation, related to a transition from a thermally excited initial state to the lowest vibrational level of the ionized final state. Alternatively, the high value of  $W_G$  itself and its increase with the temperature may be ascribed to an increase in dynamic disorder given the high mobility of the anthracene molecules. At both temperatures, the estimated value of the intramolecular reorganization energy  $\lambda$  of 150 meV is very close to the gas phase value (140 meV), at variance with observations for pentacene/HOPG [0001].<sup>31</sup> Finally, the stability of the HOMO line shape is consistent with the absence of structural transitions<sup>31</sup> within the investigated temperature range, although they still may occur at lower temperatures.

This result for the anthracene monolayer film, as well as the conservation of the gas phase vibrational energies, is



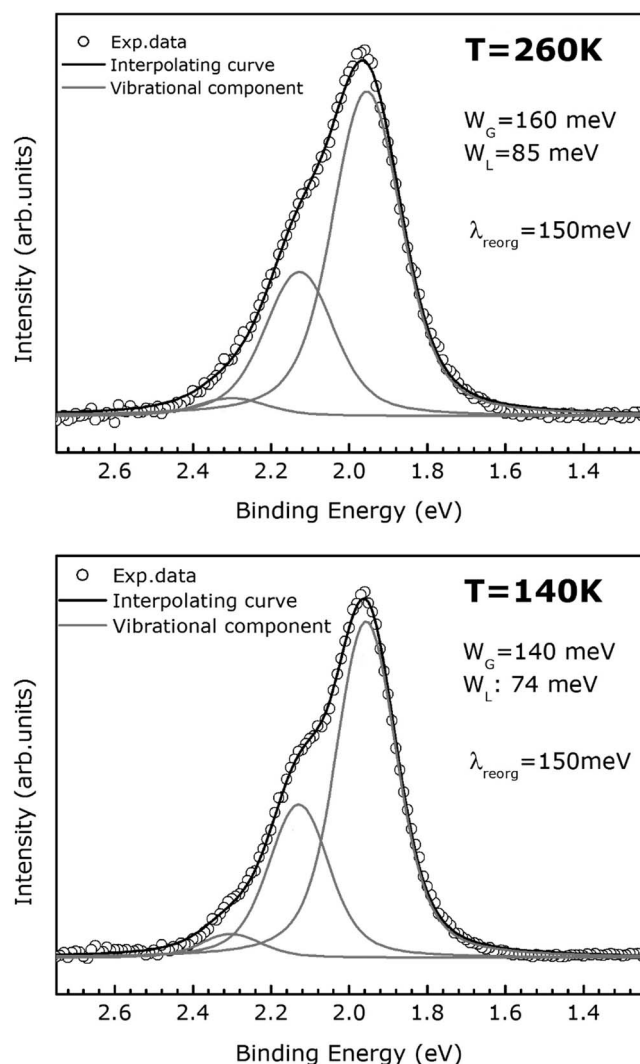


FIG. 5. Deconvolution of the angle-integrated HOMO UPS spectrum (dots) of the anthracene monolayer measured at (a) 260 and (b) 140 K with three components (gray lines). See text for details.

fully consistent with a reduced interaction as compared to pentacene molecules that interact stronger with the HOPG [0001] surface. This is expected since the anthracene monolayer desorbs at much lower temperatures than pentacene.

#### IV. CONCLUSION

In this paper, a detailed UPS investigation of anthracene mono- and multilayers on HOPG [0001] is reported. This work is proof that individual contributions to the HOMO line shape, for the same molecule on the same substrate, can be distinguished indeed. In particular, the electronic properties of each phase have been discussed with particular attention devoted to the role of the molecular orientation (“standing-up vs “flat-lying”) and structure in determining the ionization potential, band dispersions, and on-site energies due to inequivalent molecular sites. The latter is argued to be responsible for a splitting in the low-temperature “flat-lying” multilayer phase instead of surface-bulk shift due to different polarization energies. The data suggest that the role played by the surface-bulk shift in determining the HOMO line shape of organic thin films has to be reconsidered. On the other hand, a strong variation in the ionization potential with the molecular orientation by 0.9 eV cannot be explained by the dependence of the polarization energy on the aggregation state but is consistent with the recent idea of the role of the surface dipole at the vacuum/organic interface for the ionization process, important for at least some layered organic materials.

For the “flat-lying” monolayer, the HOMO vibrational fine structure is clearly revealed. The HOMO hole-vibration coupling and the intrinsic line broadening could be studied, confirming the crucial role of the molecule-substrate interaction strength for the intramolecular geometrical reorganization energy in weakly adsorbed thin aromatic molecules and of dynamic disorder for the broadening of hole energies.

Due to a marked temperature-dependent polymorphism of thin-film phases on graphite substrates combined with simple chemical and electronic structures of the anthracene molecule, a wide range of mechanisms determining transport properties of individual charge carriers can be studied. The recently renewed debate about exactly those mechanisms shows that the physics of organic thin-film materials employed in organic electronic applications is a hot topic indeed.

#### ACKNOWLEDGMENT

F.B. acknowledges support from JSPS.

\*Corresponding author; fabio@jaist.ac.jp

<sup>1</sup> *Conjugated Polymers and Molecular Interfaces: Science and Technology for Photonic and Optoelectronic Applications*, edited by W. R. Salaneck, K. Seki, A. Kahn, and J.-J. Pireaux (Marcel Dekker, New York, 2002).

<sup>2</sup> M. Halik, H. Klauk, U. Zschieschang, T. Kriem, G. Schmid, W. Radlik, and K. Wussow, *Appl. Phys. Lett.* **81**, 289 (2002).

<sup>3</sup> A. Hepp, H. Heil, W. Weise, M. Ahles, R. Schmechel, and H. von Seggern, *Phys. Rev. Lett.* **91**, 157406 (2003).

<sup>4</sup> H. Moon, R. Zeis, E. J. Borkent, C. Besnard, A. J. Lovinger, T.

Siegrist, C. Kloc, and Z. N. Bao, *J. Am. Chem. Soc.* **126**, 15322 (2004).

<sup>5</sup> J. Reynaert, D. Cheyns, D. Janssen, R. Muller, V. I. Arkhipov, J. Genoe, G. Borghs, and P. Heremans, *J. Appl. Phys.* **97**, 114501 (2005).

<sup>6</sup> C. J. Brabec, N. S. Sariciftci, and J. C. Hummelen, *Adv. Funct. Mater.* **11**, 15 (2001).

<sup>7</sup> P. Peumans, A. Yakimov, and S. R. Forrest, *J. Appl. Phys.* **93**, 3693 (2003).

<sup>8</sup> J. H. Burroughes, D. D. C. Bradley, A. R. Brown, R. N. Marks,

- K. Mackey, R. H. Friend, P. L. Burns, and A. B. Holmes, *Nature* (London) **347**, 539 (1990).
- <sup>9</sup>J. Takeya, C. Goldmann, S. Haas, K. P. Pernstich, and B. Ketterer, *J. Appl. Phys.* **94**, 5800 (2003).
- <sup>10</sup>G. Brocks, J. van den Brink, and A. F. Morpurgo, *Phys. Rev. Lett.* **93**, 146405 (2004).
- <sup>11</sup>Y. Zou, L. Kilian, A. Scholl, Th. Schmidt, R. Fink, and E. Umbach, *Surf. Sci.* **600**, 1240 (2006).
- <sup>12</sup>A. Ferretti, C. Baldacchini, A. Calzolari, R. Di Felice, A. Ruini, E. Molinari, and M. G. Betti, *Phys. Rev. Lett.* **99**, 046802 (2007).
- <sup>13</sup>H. Yamane, D. Yoshimura, E. Kawabe, R. Sumii, K. Kanai, Y. Ouchi, N. Ueno, and K. Seki, *Phys. Rev. B* **76**, 165436 (2007).
- <sup>14</sup>V. Coropceanu, M. Malagoli, D. A. da Silva Filho, N. E. Gruhn, T. G. Bill, and J. L. Brédas, *Phys. Rev. Lett.* **89**, 275503 (2002).
- <sup>15</sup>J. L. Brédas, D. Beljonne, V. Coropceanu, and J. Cornil, *Chem. Rev. (Washington, D.C.)* **104**, 4971 (2004).
- <sup>16</sup>V. Čápek and E. A. Silinsh, *Chem. Phys.* **200**, 309 (1995).
- <sup>17</sup>W. R. Salaneck, *Phys. Rev. Lett.* **40**, 60 (1978).
- <sup>18</sup>H. Fukagawa, H. Yamane, T. Kataoka, S. Kera, M. Nakamura, K. Kudo, and N. Ueno, *Phys. Rev. B* **73**, 245310 (2006).
- <sup>19</sup>A. Devos and M. Lannoo, *Phys. Rev. B* **58**, 8236 (1998).
- <sup>20</sup>T. Kato and T. Yamabe, *J. Chem. Phys.* **115**, 8592 (2001).
- <sup>21</sup>Y. Harada, H. Ozaki, and K. Ohno, *Phys. Rev. Lett.* **52**, 2269 (1984).
- <sup>22</sup>N. Sato, H. Inokuchi, and E. A. Silinsh, *Chem. Phys.* **115**, 269 (1987).
- <sup>23</sup>F. Amy, C. Chan, and A. Kahn, *Org. Electron.* **6**, 85 (2005).
- <sup>24</sup>I. G. Hill, A. Kahn, Z. G. Soos, and R. A. Pascal, *Chem. Phys. Lett.* **327**, 181 (2000).
- <sup>25</sup>R. Friedlein, X. Crispin, M. Pickholz, M. Keil, S. Stafström, and W. R. Salaneck, *Chem. Phys. Lett.* **354**, 389 (2002).
- <sup>26</sup>S. Duhm, G. Heimel, I. Salzmann, H. Glowatzki, R. Johnson, A. Vollmer, J. Rabe, and N. Koch, *Nature Mater.* **7**, 326 (2008).
- <sup>27</sup>W. Chen, H. Huang, S. Chen, Y. L. Huang, X. Y. Gao, and A. T. S. Wee, *Chem. Mater.* **20**, 7017 (2008).
- <sup>28</sup>D. A. da Silva Filho, R. Friedlein, V. Coropceanu, G. Öhrwall, W. Osikowicz, C. Suess, S. L. Sorensen, S. Svensson, W. R. Salaneck, and J. L. Brédas, *Chem. Commun. (Cambridge)* **2004**, 1702 (2004).
- <sup>29</sup>R. S. Sánchez-Carrera, V. Coropceanu, D. A. da Silva Filho, R. Friedlein, W. Osikowicz, R. Murdey, C. Suess, W. R. Salaneck, and J.-L. Brédas, *J. Phys. Chem. B* **110**, 18904 (2006).
- <sup>30</sup>S. Kera, H. Yamane, I. Sakuragi, K. K. Okudaira, and N. Ueno, *Chem. Phys. Lett.* **364**, 93 (2002).
- <sup>31</sup>H. Yamane, S. Nagamatsu, H. Fukagawa, S. Kera, R. Friedlein, K. K. Okudaira, and N. Ueno, *Phys. Rev. B* **72**, 153412 (2005).
- <sup>32</sup>N. Koch, A. Vollmer, S. Duhm, Y. Sakamoto, and T. Suzuki, *Adv. Mater.* **19**, 112 (2007).
- <sup>33</sup>N. Koch, A. Vollmer, I. Salzmann, B. Nickel, H. Weiss, and J. P. Rabe, *Phys. Rev. Lett.* **96**, 156803 (2006).
- <sup>34</sup>M. P. Seah and W. A. Dench, *Surf. Interface Anal.* **1**, 2 (1979).
- <sup>35</sup>M. S. Deleuze, A. F. Trofimov, and L. S. Cederbaum, *J. Chem. Phys.* **115**, 5859 (2001).
- <sup>36</sup>M. B. Casu, Y. Zou, S. Kera, D. Batchelor, Th. Schmidt, and E. Umbach, *Phys. Rev. B* **76**, 193311 (2007).
- <sup>37</sup>R. Friedlein, X. Crispin, C. D. Simpson, D. M. Watson, F. Jäckel, W. Osikowicz, S. Marciniak, M. P. de Jong, P. Samorí, S. K. M. Jönsson, M. Fahlman, K. Müllen, J. P. Rabe, and W. R. Salaneck, *Phys. Rev. B* **68**, 195414 (2003).
- <sup>38</sup>X. Crispin, J. Cornil, R. Friedlein, K. K. Okudaira, V. Lemaure, A. Crispin, G. Kestemont, M. Lehmann, M. Fahlman, R. Lazzaroni, Y. Geerts, G. Wendin, N. Ueno, J.-L. Brédas, and W. R. Salaneck, *J. Am. Chem. Soc.* **126**, 11889 (2004).
- <sup>39</sup>W. Dou, N. Li, D. Guan, F. Song, H. Huang, H. Zhang, H. Li, P. He, S. Baoa, Q. Chen, and W. Zhou, *J. Chem. Phys.* **127**, 224709 (2007).
- <sup>40</sup>H. Yoshida and N. Sato, *Phys. Rev. B* **77**, 235205 (2008).
- <sup>41</sup>H. Yamane, S. Kera, K. K. Okudaira, D. Yoshimura, K. Seki, and N. Ueno, *Phys. Rev. B* **68**, 033102 (2003).
- <sup>42</sup>N. Ueno and S. Kera, *Prog. Surf. Sci.* **83**, 490 (2008).
- <sup>43</sup>V. Palermo, M. Palma, Ž. Tomović, M. D. Watson, R. Friedlein, K. Müllen, and P. Samorí, *ChemPhysChem* **6**, 2371 (2005).
- <sup>44</sup>H. Yamane, Y. Yabuuchi, H. Fukagawa, S. Kera, K. K. Okudaira, and N. Ueno, *J. Appl. Phys.* **99**, 093705 (2006).
- <sup>45</sup>P. B. Paramonov, V. Coropceanu, and J.-L. Brédas, *Phys. Rev. B* **78**, 041403(R) (2008).